Journal Pre-proof

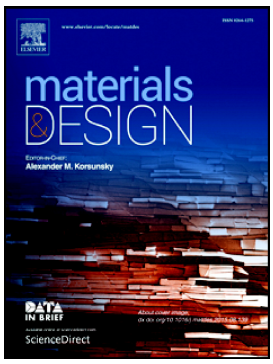

3D printing of very soft elastomer and sacrificial carbohydrate glass/elastomer structures for robotic applications

Armita Hamidi, Yonas Tadesse

PII: S0264-1275(19)30762-2

DOI: https://doi.org/10.1016/j.matdes.2019.108324

Reference: JMADE 108324

To appear in: *Materials & Design*

Received date: 2 August 2019

Revised date: 29 October 2019

Accepted date: 30 October 2019

Please cite this article as: A. Hamidi and Y. Tadesse, 3D printing of very soft elastomer and sacrificial carbohydrate glass/elastomer structures for robotic applications, *Materials & Design*(2019), https://doi.org/10.1016/j.matdes.2019.108324

3D printing of very soft elastomer and sacrificial carbohydrate glass/elastomer structures for robotic applications

Armita Hamidi[1*] and Yonas Tadesse[2*]

[1]armita.hamidi@utdallas.edu, [2]Yonas.Tadesse@utdallas.edu,

[*] Humanoid, Biorobotics and Smart Systems (HBS Lab)
Mechanical Engineering Department,
Erik Jonsson School of Engineering and Computer Science,
The University of Texas at Dallas (UTD),
800 West Campbell Rd., Richardson, TX75080-3021

Abstract

Recently, soft materials such as silicone elastomers are widely used in soft robotics due to their high flexibility and safe physical interaction with humans. Focusing on three aspects—*highly elastic materials, sacrificial materials, and actuation units*, we aim to develop an additive manufacturing strategy that allows the fabrication of highly elastic soft structures more efficiently. First, silicone thinner is used to tailor the mechanical properties of the soft silicone elastomer. We found out that adding 20% volume thinner to the silicone improved the ultimate tensile elongation of 3D printed silicone samples upto 1260%, which is the highest among all the 3D printed soft materials previously reported. However, in a cyclic tensile test, this strain is not achieved; instead, the maximum strain was 600 %. Second, carbohydrate glasses are introduced as sacrificial materials for 3D printing silicone with hollow channels. Few configurations of pneumatic and hydraulic actuators are developed by forming channels in the silicone elastomer via 3D printed sacrificial carbohydrate structures and subsequently dissolving. The 3D printed structures actuated successfully to get morphed shapes, which showed that our method is effective for manufacturing of functional soft robotic structures.

Keywords: Additive manufacturing, soft elastomer, elasticity, sacrificial material, carbohydrate glass, soft actuator

1. Introduction

In recent years, soft robots have been gaining popularity due to their ability to interact safely with humans and ability to function in an inaccessible environment [1]. The characterization of these soft robots is extremely dependent on the overall design and the materials used for fabricating the structure. Rubber-like materials that are inherently non-linear, viscoelastic, homogeneous materials are suitable for soft robotics applications [2]. In general, soft materials used in robots are commonly composed of hydrogels [3, 4] and elastomers [5-7]. Elastomers are appropriate for fabricating soft robots and actuators due to their ability to restore their shapes after high deformations. As a typical example, a soft pneumatic actuator can sustain high elongation at high air pressure due to the high elasticity of the elastomer.

Additionally, elastomers have lower elastic modulus (E<1MPa), which make them similar to biological tissues and cells [8] and suitable for stretchable electronics. However, casting these materials is time consuming, as it requires multiple steps including preparing molds and coating with release agents as well as long curing time [9, 10]. Moreover, this method is not suitable for producing parts having complex internal geometries. Additive manufacturing (AM) has the potential to replace this traditional casting technique and enables the creation of complex and novel designs. The development of this type of manufacturing method will facilitate the direct fabrication of soft robots with distinct functional elements. It can also be used for creating gradual transition from soft to hard components [11].

Recently, several AM techniques and processing methods have been developed for printing silicone and other soft materials. Stereolithography (SLA) [12, 13], digital light processing (DLP) printing [14], selective laser sintering (SLS) [9, 15], photopolymer jetting [16], fused deposition modelling (FDM) [17, 18] and direct ink writing (DIW) [19] have been used for 3D printing soft materials. These techniques are explained and compared in supplementary file in table S1. The table includes the detailed information on the materials, resolution, elongation, curing method, shore hardness and modulus of each method. Among all these techniques, FDM and DIW are the most common methods due to their low material cost and ease of use. However, FDM has constraints regarding material compatibility. In the FDM process, the material should be prepared and inserted in the machine as a solid filament and only thermoplastic polymers (ABS, PLA, PETG, TPE, etc.) can be used in this technology due to the heating and cooling process [11]. Liquid forms such as RTV silicones and gels cannot be used in FDM, which is one of the problems of this technology. DIW is another technique, which is widely used for printing hydrogel [20] and silicone [21, 22]. This technique is also further developed for 3D printing other types of gels [23]. Yet, preparing a customized ink (or solution) that has proper rheological properties for extrusion and that can provide expected mechanical properties after rapid solidification is challenging. Therefore, for developing a proper silicone printing, the polymerization mechanism of silicone should be understood in terms of rheological and mechanical properties [24].

Understanding the material properties, Liravi et al. [25] optimized the silicone printing accuracy and speed in one and two-dimensional levels (line and plane) by a hybrid 3D printing method that combined material extrusion and material jetting techniques. They used one-part UV-curable silicone in their system, which resulted in 600% ultimate tensile strain. The rheological properties (such as shear yield stress and viscosity) of the silicone elastomer ink during and after the extrusion should be suitable for smooth flow through a nozzle and for curing rapidly after extrusion. Otherwise, the 3D printed structure can easily deform or collapse. Weak intermolecular forces and the viscoelastic behavior of elastomers pose a problem for printing processes. Therefore, there is still a need to develop a proper technique, which can be used to print all complicated, overhanging or hollow structures with soft elastomers.

In single extruder FDM 3D printers, the same material can be used for building supports. This technique is not applicable to internal cavities where the support structure is trapped inside and cannot be removed. Additionally, removal of material is not easy and occasionally, it leaves marks on the surface where it is attached. In conventional 3D printing, a different support material is used to print features with overhangs or cavities. There are two major plastics used as dissolvable support structures in desktop 3D printers, polyvinyl alcohol (PVA) and high impact polystyrene (HIPS), and both have their own limitations. Although PVA can be removed by water, it is sensitive to ambient conditions such as moisture and temperature and does not stick well to the 3D printed surfaces. HIPS, on the other hand, should stay in chemical bath for several hours to be dissolved. In AM of silicone, PVA (in FDM printers) [26] and wax (in photopolymer printing) [27, 28] have been proposed and

studied for use as support materials. In another method called freeform reversible embedding (FRE), silicone is printed and cured simultaneously inside a vat of another material, which acts as a support bath [29-31]. A soft robot [32] and organ-tissue structures with vascular networks [33] are fabricated by the embedded 3D printing technique using removable fluid (ink). Most of the other implemented techniques for printing soft structures are support free [34, 35]. Plott and Shih [35] presented a technique for bridging horizontal ledges to fabricate pneumatic actuators using extrusion-based AM of moisture-cured silicone. They used the moisture-cured silicone in their DIW 3D printing setup and fabricated a pneumatic soft actuator. Their experiments showed that the success of this procedure is dependent on the number of bridge layers and their thickness, which can limit the geometry and size of the part. Therefore, bridging solves one of the issues in printing silicone. Despite the benefit, this method cannot be used for fabricating porous structures. Walker et al.[36] adjusted transient curing properties (elastic modulus, loss modulus, and yield stress) for thermoset silicone in order to 3D print structures without utilizing any support material or fluid bath. However, their method results in limited geometries. They showed that this method can be used for manufacturing parts with less than 35 degree (from the vertical) overhanging features. Thus, there is still a lack of suitable support material in 3D printing silicone.

In 3D printing silicone with the use of support material, several parameters should be considered for choosing the optimal support material. One of the key elements is having a strong adhesion between support material and silicone. This improves the quality of printing. Another key element is the total removal of the support structure, which should not be difficult and time-consuming especially inside deep cavities or channels. Considering all the above aspects, this paper presents the usage of 3D printed carbohydrate glass (i.e. sugar) as a sacrificial structure in AM of very soft material. Sugar is a low-cost available material that can dissolve easily in water and is biodegradable. In a related study, Godoi et al.[37] summarized some of the techniques used for carbohydrate printing and their application in the food industry. In another study, Song et al. [38] used sugar particles as a foaming agent in stereolithography to make porous structures. The porous structures were fabricated from sugar mixed with a photo-curable resin by a stereolithographic 3D printer, and then the printed structures were dipped into hot water to dissolve sugar and increase the overall porosity. The application of sugar printing in fabricating vascular networks and tissue engineering is also reported in several previous studies [39-43]. Miller et al. [43] used a 3D printed carbohydrate glass lattice with a size of 20mm×10mm×2.4mm, as a sacrificial template for casting 3D-vascular architectures. Similarly, He et al. [44] investigated the fabrication of microchannels for microfluidic chip devices by testing different types of sugar in a 3D printer setup. They poured PDMS on a 25mm×25mm×2.2 mm sugar structure, and cured it in an oven and then, kept it in boiling water to dissolve the sugar and form a microfluidic chip. In recent years, several systems for 3D printing molten carbohydrate glass are also designed and developed [45, 46].

In this paper, we aim to establish an AM strategy that can accelerate producing highly elastic soft structures. A very soft elastomer substrate is used in a custom-made 3D printing setup to create complex objects. The properties of molten carbohydrates are studied for employing as sacrificial support materials in 3D printing of silicone. We refere the support materials as carbohydrates rather than sugar. This is because carbohydrates include sugar alcohol, table sugar and any mixture of them. In our AM process, the molten carbohydrate is extruded first and it is solidified at the room temperature and becoming stiff enough to hold the soft silicone material. Moreover, it sticks well to the silicone during the printing process and it can be easily removed by submerging in warm water. These properties of sugar, besides its low cost, make it a suitable candidate as a support material for 3D printing soft mechanical structures. Therefore, the 3D printed carbohydrate glass along with very

soft elastomer is used to build a soft robotic structure (shown in Fig. 1) that can be pneumatically actuated. The sugar embedded between the 3D printed silicone layers is removed by keeping the composite in warm water to obtain the hollow channels. Molten sugar is selected rather than solid sugar for our current study because complex geometries can be easily created by using the molten sugar in our setup. To summarize, the highlights of this study are:

- Material processing (printing) parameters in additive manufacturing of silicone are investigated in this work. The result of this study allows the fabrication of highly elastic soft structures more efficiently by eliminating the need for assembly and post-processing (Fig.1).
- 3D printed silicone samples reached 1260 % elongation in uniaxial tensile tests, which is the highest strain reported for elastomers. Moreover, extensive material characterization, i.e. microscopic images, atomic force microscopy (AFM), tensile test and cyclic extension tests are performed on the fabricated soft samples.
- Soft pneumatic and hydraulic actuators are fabricated in this work to demonstrate the potential application of our method (3D printing soft material with carbohydrate glass) for creating functional robotic structures.

The rest of the paper is organized as follows. In Section 2, the 3D printer setups and the materials are described. Properties of three different types of sugar used in the printer setup are discussed in this section. We used sugar and carbohydrate glass alternatively in this paper when discussing about support materials. The properties of the 3D printed silicone, the effects of adding thinner and experimental results are discussed in Section 3. We also showed how 3D printing silicone along with sacrificial carbohydrate glass could be used to build actuators in this section. Finally, Section 4 includes the conclusion and future work.

2. Materials and 3D printer setup

2.1. Preparing silicone for 3D printing

A platinum-cured silicone, Ecoflex 0010 (Smooth-On, Inc.), was used in this study. This kind of room temperature vulcanizing (RTV) silicone is suitable for a variety of applications including making prosthetic and orthotic devices. The material consists of a two-part solution, part A and B that are mixed in a 1:1 volume ratio prior to injecting to an extruder. Due to the relatively low density (1040.2 kg/m^3) and good flowability of the mixture (viscosity in the range of 140 Poise)[47], such silicone is a good candidate for extrusion-based 3D printing. For obtaining lower viscosity and easier extrusion, we added silicone thinner (Silicone Thinner™, Smooth-On, Inc.) to the silicone before it cured. Silicone thinner is a non-reactive silicone fluid that lowers the viscosity of part A and B during mixing [48] and allows the mixture to flow easily through the extruder.

Two existing open source 3D printers (Prusa 8" i3v kit, Maker Farm) are modified to print silicone and carbohydrate glass. Both printers have glass beds, which can be transferred easily from one setup to the other without detaching the printed structure. Hence, both setup can be used in printing a particular design. A single paste extruder (DISCOV3RY, Structur3D Printing) is modified to 3D print Ecoflex 0010 as shown in Fig. 2(a). The motorized paste extruder is shown in the schematic diagram in Fig. 2(b). It uses a 60 cc syringe, plastic connectors and 30.5 cm long plastic feeding pipe with an inner diameter of 3.2 mm. A plastic nozzle is attached to the end of the tube for controlling the resolution. The material in the syringe is pushed through the tube due to the pressure of the plunger, which is driven by a stepper motor. Samples were successfully printed with 0.8, 0.6 and 0.4 mm (inner diameter, *d*) nozzles. The smallest nozzle size (0.4 mm) was used to print structures with high precision for the rest of the study. The process parameters for silicone extrusion are obtained from our previous work [49], shown in table 1. A single layer thickness of a 3D printed sample is 0.5mm after

curing. For measuring the dimensional accuracy, a 100mm×100mm×15mm cubical structure is 3D printed, and each side is measured and compared to the initial design. The measured error was 0.4 mm in x and y directions and 0.1mm in the Z direction, which is less than 1% error in all directions.

2.2. Preparing carbohydrate glass for 3D printing

Carbohydrate glass(sugar) is used as a sacrificial material for AM of silicone in this study due to solubility in water, compatibility and low cost. Most of the carbohydrate glass mixtures can be prepared by melting them at temperatures higher than 90˚C to lower the viscosity in order to pass through the nozzle for printing. If the extruded sugar cools to the glass transition temperature, it will form into a solid shape and this is beneficial for 3D printing. The melting and glass transition temperatures for several sugar compounds are presented in table 2 for more detailed information. The process of preparing the molten carbohydrate is very important to prevent crystallization and forming solid particles within the flow during extrusion. Heating sugar to temperatures higher than its melting temperature will help to prevent crystallization. However, this temperature is limited due to the burning and degradation of sugar (~176˚C). Based on these properties and the literature, three types of carbohydrates, *table sugar, sugar/syrup mixture, and maltitol* were prepared for printing. A pneumatic system consisting of a pressure regulator and pneumatic fluid dispenser is used in the sugar 3D printing setup (Fig. 2(c)). The extruder is a modified design of the system presented in [42] as shown in Fig. 2(d). A dispensing apparatus with a 0.6 mm nozzle diameter is made for carrying and extruding a molten sugar. The molten sugar is kept at 120˚C inside the syringe, heated by passing current through the heating coils wrapped around its barrel.

For the first type, table sugar (sucrose), the crystals were heated to 160˚C in a heater until they are melted. Then, the molten sugar was poured into a hot reservoir (syringe container). Based on our previous work related to sugar printing [50], sugar properties are difficult to control during printing, and consequently, it limits maintaining the geometrical accuracy. The nozzle would frequently clog if the temperature decreases due to the crystallization of sugar. Initial crystallization starts with developing nuclei, which are the initial forms of crystals. But they are undetectable before the crystals grow to a size where they can be observed. During 3D printing with sugar, if the nozzle temperature drops, the material extrusion rate starts decreasing until the extrusion nozzle clogs due to the growth of the sugar crystals. Crystallization is accelerated by shear, which is unavoidable in extrusion processes but is preventable by maintaining the material above its crystalline melting point (~160 ˚C). On the other hand, increasing the temperature will degrade and oxidize the sugar. Therefore, another printing material (the second type) was prepared by mixing white table sugar (62% by weight), syrup (31% by weight), and water (6% by weight). The presence of water and corn syrup (contributing a mixture of glucose, fructose, and other saccharides) in the sugar mixture lowers its melting temperature and glass transition temperature and delays the crystallization [51]. The mixture was continuously heated to 154 ˚C and poured in the hot reservoir after cooling down to 140˚C. In this case, adding syrup and water to the sugar mixture prevented the crystallization as also observed in [33] and increased the quality (accuracy, precision, and dimensional tolerances) of 3D printed carbohydrate glass. However, controlling the flow of the molten material due to the rapid changes of the viscosity with temperature (Fig. 3) is more challenging particularly if a higher rate of heat loss occurs during printing. In addition, the mixture of sugar and syrup has a higher viscosity than sugar (i.e. 5000 cP at 110 ˚C for the mixture of sugar and syrup while it is less than 2000 cP for the sugar), and consequently, less flow-ability. The results of 3D printing with sugar and sugar/syrup mixture are shown in Fig. S1. The third and final carbohydrate candidate for 3D printing was maltitol, which is a sugar alcohol made of glucose and sorbitol (differs in chain length with sugar, which has two fewer

hydrogen atoms). Maltitol has a melting point at 145˚C, it has a stable flow properties and low cost [44].

In the 3D printing process of carbohydrate glass (sugar), three processing parameters, namely temperature, viscosity, and pressure are dependent on each other and should be calibrated. Several experiments were performed in this work to find the relation between printing parameters. Viscosity measurements were done by Brookfield DVT2 viscometer (with LV-04 (64) cylindrical spindle) at 25 rpm and the results are presented in Fig. 3. The results show that viscosity is decreasing exponentially as the temperature is increasing for all the three types of carbohydrates. This behavior can be described by equation 1:

$$\nu = ae^{bT} \quad (1)$$

Where ν(Poise) is the viscosity, T (˚C) is the temperature, a and b are the constants. The calculated constants obtained by model fitting of the viscosity data are shown in table S2.

The viscosity of all tested carbohydrates remains below 250 Poise for the temperature range of 60˚C to 140˚C. During the printing process with carbohydrate glass, the nozzle and reservoir temperatures were kept at almost 120˚C by uniformly heating with 28W heating wires. A 100 kPa pressure was applied by the pneumatic system from the top side of the syringe and the molten carbohydrate was extruded, and then quickly solidified at room temperature. We empirically observed that for obtaining the best result in printing structures with sugar/syrup mixture and maltitol, the nozzle translation speed should be adjusted to 5mm/s and 10mm/s, respectively. The silicone channels with minimum 5mm width were successfully printed using this method for both sugar/syrup mixture and maltitol (video S1). Yet, printing smaller structures is difficult with the current setup, since the difference between the extruded sugar filament diameter and the nozzle diameter (at a constant feed rate) increases when the nozzle diameter is greater than 0.4 mm [45].

The theoretical relationship between the printing speed and the diameter of the extruded carbohydrate glass (sugar) for a constant nozzle size is described in equation 2 [43]:

$$D = C/V^{0.5} \quad (2)$$

Where D is the diameter of the extruded carbohydrate glass, V is the translation speed of the extruder and C is a constant that depends on the nozzle diameter and pressure. This equation is used to find the relationship between the translation speed and the extruded sugar diameter (Fig S3). Gelber et al. [45] observed that the width of the extruded carbohydrate filament increases for higher nozzle sizes owing to the surface tension and forces generated by viscous expansion. Due to the nozzle size, the lowest layer height of the 3D printed carbohydrate glass that can be achieved in our setup is 0.6 mm, while the thickness of the layers is occasionally reached more than 1 mm, since sugar layer spread on the surface. Decreasing the nozzle diameter can resolve this problem, but clogging may occur more often. Our main focus in this work is to demonstrate the application of carbohydrate glass 3D printing in AM of soft actuators. Improving the carbohydrate glass printing precision by both empirical and analytical relations will be the focus of our future study using similar methods as demonstrated in reference [37].

We observed that maltitol properties are easier to control during printing and can produce structures with better dimensional accuracy for small-scale prints. Maltitol can be also reheated and re-used in 3D printing. Reheating maltitol removes the water content and improves the extrusion process of the material. This process can be continued before the material oxidizes and burns as shown in Fig. 4.

As stated earlier, for both setups (elastomer and carbohydrate), an open source printing software (Repetier-Host) is modified to control the printer sections (the xyz stage, the heaters, the extruder, and the pneumatic device). A 3D model was created with a commercial 3D modeling software and the stereolithography (STL) file was sent to the 3D printer software. The 3D printing software 'Slic3r' was used for converting the print head paths into machine control code (G code). Finally, the control code was reviewed, revised and uploaded to Repetier-Host to initiate the process. The best 3D printing parameters for each material are achieved based on several experiments (table 1).

3. Results and discussion

In this section, we present the results for the soft material characterization as well as the 3D printed structures. These results demonstrate the physical properties and surface morphologies of the 3D printed samples obtained from optical microscopy and atomic force microscopy (AFM) while the mechanical properties of the parts are investigated using standard uniaxial tensile test.

3.1. Characterization of the 3D printed silicone

The curing rate of RTV silicone is heavily dependent on the temperature and the amount of the material. In order to shorten the curing time and to avoid self-collapsing while maintaining enough bonding between the layers, the printer bed temperature was set to maintain at 100˚C. This temperature helps the chemical bonding (Fig. 5(a)) reaches a steady state as in few seconds (~ 1-2 s) after the material is extruded. Once exposed to the heat, the interlayer crosslinking occurs chemically and bonds adjacent layers together. The strength of these interfaces is important and it is dependent on both geometric parameters and on the chemical bonding within the material [52]. For further studies, the microscopic images of the 3D printed bonded layers of Ecoflex 0010 mixed with 20% of thinner, were taken by Leica DMi1(Leica Microsystems Inc). A 6mm×5mm×4mm printed section was taken from the side length of the 3D printed sample as shown in Fig. 5(b). The image of this 3D printed piece is shown in Fig. 5(c). The optical microscopic images of the 3D printed surface and cross section with 5x magnification are shown in Fig. 5(d)& (e), respectively. The surface roughness is also examined to characterize the same 3D printed silicone part and reveal the structural appearance and the asperity of the surface. In this work, atomic force microscopy (AFM) is used to test the quality of the surface based on ISO 25178 standard (Fig.5(f) & (g)) by Tosca^{TM} 400.

Surface quality is another important physical property that may affect the accuracy, cost, and functionality of the part. Since the surface property can strongly determine properties such as mechanical, biological, optical, acoustic and electronic properties of the material [53]. In general, the surface roughness is described by surface arithmetical mean height (S_a) and root mean square (S_q) of the extracted surface data (Fig 5.(f) & (g)). This is calculated using equations 3 and 4, where Z is the surface height, A is the surface area, x and y are length and width of the scanned structure. For a 20μm x 20μm cross sectional area (as shown in Fig.5 (g)), S_a and S_q are determined as 0.0028 μm (2.8 nm) and 0.00346 μm (3.5 nm) respectively. The results of AFM show a uniform interlayer structure inside the material, while the smoothness of the silicone surface is comparable to the acetone polished molds' surfaces shown in the scientific report from He et al. [54].

$$S_a = \iint_A |Z(x,y)| dxdy \tag{3}$$

$$S_q = \sqrt{\frac{1}{A}\iint_A Z^2(x,y) dxdy} \tag{4}$$

3.2. Effect of different percentage of silicone thinner mixed with silicone

The influence of thinner on deformation characteristics of silicone is studied by conducting several tensile tests and measuring the stress-strain behavior of samples fabricated with different thinner concentration. All the samples for the tensile test were designed based on ASTM dog bone structure D412 type C with an overall size of 33mm×25mm×4mm [55]. The test specimen geometry was defined in a CAD file (Creo Parametric 2.0, PTC), exported as a STL file for loading into the 3D printer slicing software package (Slic3r) and 3D printed using our setup. The 3D printed dog bone samples (three samples for each composition) are shown in Fig. 6(a) & (b). We investigated the mechanical properties of 3D printed silicone samples mixed with 2 different volume percentages of thinner agent and compared with the same material fabricated by casting in a 3D printed mold. The tensile test was performed using high resolution Instron Universal Tensile system with a 10 kN load cell (2580 series) and at a rate of 500 mm per min (Fig. 6(c)). The test data was collected using Bluehill software and analysis was performed. Finally, a rectangular chamber (thin wall) with 80 mm in length and 3 mm in width was 3D printed with Ecoflex 0010 mixed with 20% and 25% thinner agent and compared. According to Fig. 6(d), Ecoflex 0010 mixed with 20% thinner has better properties for 3D printing especially for fabricating soft structures that contain thin walls. The importance of silicone composite is also studied in another intricate geometry. As shown in Fig. 7(a), a structure with complex open channels is 3D printed with Ecoflex 0010 mixed with 20% thinner agent and stretched (Fig. 7(b)). The channels were designed on the surface with 200 μm width and fabricated without any imperfection (i.e. over and under extrusion).

Fig. 8 (a), (b), (c) & (d) show the tensile test results of cast Ecoflex 0010 mixed with 0 to 25% of thinner agent. As a general trend, ultimate tear and tensile strength are reduced in proportion to the amount of thinner added in the silicone. The results of 3D printed Ecoflex 0010 mixed with 20% and 25% thinner are presented in Fig. 8(e) & (f). These results have a similar trend to the casted samples and demonstrate that lower force is needed to stretch the samples when the percentage of thinner increases. Also, the strain is improved slightly compared to the casted samples. Moreover, both cast and 3D printed samples of Ecoflex 0010, for example, 25% silicone thinner, did not tear during the test, but due to the limitation of the Instron machine for the extension, we stopped the test once the maximum displacement was reached. Other percentages of thinner agent could not be fabricated and compared due to the specific flow properties required in the setup for 3D printing soft samples. The plot corresponding to axial force–elongation curves, Fig. 9 (a) demonstrates that the force required to stretch the sample reduces when the percentage of thinner increases. The maximum applied force to the samples is 14N and the load cell had high resolution to capture the incremental load. The stress-strain results of the samples are shown in the supplementary Fig. S4. The results showed that the modulus at 100% strain (100% E), decreased from 0.02 MPa for cast Ecoflex 0010 with 0% thinner to 0.01 MPa and 0.008 MPa for 3D printed samples with 20% and 25% thinner, respectively (Fig. S5). 3D printing silicone with higher percentages of thinner is limited to 25% thinner, because adding higher percentages of thinner makes the mixture improper for printing. Furthermore, Ecoflex 0010 surface is oily and sticky. Thus, corn starch is used to make the surface less sticky (reduce tackiness) after preparing all the samples. Our results in this section can be compared to previously reported 3D printed highly stretchable and UV curable elastomer used in the DLP 3D printing technique that stretched up to 1100% [14]. We showed a remarkable strain in our 3D printed samples, which can reach up to 1260% strain (Fig.9(b)). This is a consequence of adding the additives in the silicone elastomer and the printing temperature utilized for the dog bone sample during printing. The high strain was obtained from three samples and it is the average value for all the three. In Fig.9(b), we

tried to compare the maximum elongation of 3D printed soft material (PDMS, TPU, SUV elastomer, and our composition).

3.3. Cyclic test

For further characterization, cyclic strain-stress tests were performed for 5 cycles on each sample. The cast samples with different percentage of thinner are tested to study the effect of adding thinner in the cyclic response (Fig. 10 (a)-((d)). Adding higher thinner percentages to the silicone reduced the stress magnitude at constant strain, but did not affect the cyclic behavior of the material (hysteresis). Stress softening phenomenon is observed, which is known as the Mullins effect[56]. For all samples, the results show that at a constant displacement amplitude, the stress decreases between successive loading cycles during the first and second cycles. The stress variations become negligible after the third cycle, which is a common behavior for soft materials [56]. The hysteresis in the first cycle increases as we increase the strain in the 3D printed samples. This test is repeated for 3D printed samples at maximum strains equal to 300%, 400% and 500% as shown in Fig.10 (d), Fig. 10(e) and Fig. 10(f), respectively. The strain rate is set to 500 mm per min in all cyclic tests. The results proved that repeatable stress cycles and low hysteresis loops are observed after several cycles. Lifetime test is also performed on the 3D printed sample with Ecoflex 0010 mixed with 20% of thinner. In this case, the sample is stretched to 400% strain for 40 times at a rate of 500mm per min without failure (Fig. 10(h)). This shows that this sample is reliable for repeated use. The modulus of resilience is a key factor that is particularly important for soft robotic materials. This is the maximum energy that can be elastically recovered during a loading cycle to return the robot to its original form [11]. The result of this study can prove that the elastic modulus obtained through the tensile loading and unloading curves is appropriate for enabling large, recoverable local strain differentials using small force/stress. In addition, the cyclic test illustrates that our material has good resistance to failure and fatigue. Representative time-domain cyclic force is shown in supplementary figure S6, showing the profile of the force in the forward and return cycles.

3.4. 3D printed soft actuator structures

In this paper, we showed several 3D printed soft actuating structures and analyzed their performance. The fabrication process is simplified to three major steps, which are design, 3D printing, and installing tubes or embedding the actuators (depending on the selected actuation technology). Two methods are used to test the ability of the carbohydrate glass to form channels. In the first method, the carbohydrate glass and the bottom section of the silicone structure are printed separately, then the carbohydrate glass is placed on the intended location on the surface of the 3D printed silicone. Then, the surface is covered by 3D printing another layer of silicone on the top. One illustration of this process is shown in Fig. 11(a-d). The trajectory of the print head is controlled and adjusted according to the geometry of the printed materials by the G-code. As it is shown in Fig. 11(e), the hollow channels are formed in the 3D printed soft elastomer by embedding a 3D printed carbohydrate glass in-between silicone during printing. The sugar is dissolved by keeping the printed structure in a warm water bath. This process was discussed earlier in the schematic diagram Fig.1.

In the second method, a silicone layer is 3D printed on a movable build plate (glass material), then the build plate is taken to the sugar printer setup to print the sugar structure on top of it. The assembly is taken back to the silicone print setup and silicone is printed at the top. This approach uses the two printer setups (Fig. 2(a) & (c)) at the same time. Similar to the first method, the printed structure is kept in a warm water until the sacrificial carbohydrate structure is removed completely. Using the second method, a soft pneumatic actuator with a single chamber was created. The actuator had a 76mm×16mm×16 mm shelled structure with a wall thickness of 3 mm, shown in Fig. 12(a). The chamber was 3D printed without the top surface (the same structure shown in Fig. 6(d)) and it was

transferred to the sugar 3D printer setup, to be filled with carbohydrate glass. For the initial demonstration, the two setups are kept close to each other, but they can also be combined as one setup, which will be presented in our future work. Finally, the structure attached to the build plate was brought back to the elastomer 3D printer and sealed by printing silicone on top of the sugar structure. The carbohydrate glass was dissolved by water penetrated inside the structure through a hole made for installing a pneumatic tube. A pressure test is performed by increasing the air pressure inside the chamber until it burst. This experiment was conducted as shown in Fig. 12(b); a solenoid valve is used for supplying air inside the channel at 70 kPa. The length of the chamber reached 150mm before it burst, which is more than twice its original length (Fig. 12 (c)&(d)). This test reveals that the inter-layer bonding is strong and sustain large deformation. Therefore, the manufacturing method presented here results in a functional pneumatic actuators/structures, which are made by 3D printed silicone and sacrificial carbohydrate glass. Another soft robotic structure inspired by [56] is designed (Fig. 12(e)) and 3D printed with the same procedure as shown in Fig.12(f). After removing sugar from the channels, the actuator bent to 70˚ when water is injected inside the structure (Fig. 12(g)). Such method is typyically called hydraulic actuation. This demonstrates that our fabrication approach is versatile to use in fluidic actuators (pneumatic and hydraulic) that are basic structures of soft robots.

4. Conclusion and future work

In this work, an inexpensive custom-made 3D printing setup is developed and utilized for fabricating different functional structures. RTV silicone properties are controlled by adding silicone thinner and heating at 100˚C during printing. The 3D printed elastomer in this work has the highest strain (1260%) as compared to previous reports (Fig.9 (b)) and 0.008 MPa elastic modulus at 100% strain. A comparison of the mechanical properties obtained from the study is done between the 3D printed and cast elastomer with different percentages of thinner from 0% to 25%. More importantly, 3D printed carbohydrate glass structures is used as a sacrificial structure to form hollow channels in silicone, for the realization of pneumatic and hydraulic soft actuators. 3D printing stretchable elastomeric structures with carbohydrate glass is important and can be used easily and safely in 3D printers used at schools particularly for educational purposes. This printing strategy with carbohydrate glass is beneficial as the employed material is organic, inexpensive and commercially available. Sugar is also a suitable replacement for hazardous chemicals and support structures used in current 3D printers. Future work includes working on a small heating system for curing silicone (such as laser or radiation device) that can be attached close to the nozzle in order to heat each layer right after it extrudes. In that case, both materials, silicone, and sugar can be built in a common build plate. The presented method can also be further developed for implementing in multi material 3D printing.

Acknowledgment

The authors would like to acknowledge the support of the Office of Naval Research (ONR), Young Investigator Program, under Grant No. N00014-15-1-2503. The authors would like to thank Professor Hongbing Lu, associate department head of mechanical engineering and his student, Sadeq Malakooti for their collaboration in performing tensile tests. The authors also like to acknowledge Pooyan Javadzadeh for his help in preparing sugar setup.

References:

[1] J.C. Case, E.L. White, R.K. Kramer, Soft Material Characterization for Robotic Applications, Soft Robot 2(2) (2015) 80-87.
[2] N. Elango, A.A.M. Faudzi, A review article: investigations on soft materials for soft robot manipulations, Int J Adv Manuf Tech 80(5-8) (2015) 1027-1037.
[3] H. Li, G. Go, S.Y. Ko, J.O. Park, S. Park, Magnetic actuated pH-responsive hydrogel-based soft micro-robot for targeted drug delivery, Smart Mater Struct 25(2) (2016).
[4] D. Morales, E. Palleau, M.D. Dickey, O.D. Velev, Electro-actuated hydrogel walkers with dual responsive legs, Soft Matter 10(9) (2014) 1337-1348.
[5] L. Hines, K. Petersen, G.Z. Lum, M. Sitti, Soft Actuators for Small-Scale Robotics, Adv Mater 29(13) (2017).
[6] H.T. Lin, G.G. Leisk, B. Trimmer, GoQBot: a caterpillar-inspired soft-bodied rolling robot, Bioinspir Biomim 6(2) (2011).
[7] C.D. Onal, X. Chen, G.M. Whitesides, D. Rus, Soft Mobile Robots with On-Board Chemical Pressure Generation, Springer Trac Adv Ro 100 (2017).
[8] R. Akhtar, M.J. Sherratt, J.K. Cruickshank, B. Derby, Characterizing the elastic properties of tissues, Mater Today 14(3) (2011) 96-105.
[9] R.V. Martinez, C.R. Fish, X. Chen, G.M. Whitesides, Elastomeric Origami: Programmable Paper-Elastomer Composites as Pneumatic Actuators, Adv Funct Mater 22(7) (2012) 1376-1384.
[10] A.A. Calderon, J.C. Ugalde, J.C. Zagal, N.O. Perez-Arancibia, Design, Fabrication and Control of a Multi-Material-Multi-Actuator Soft Robot Inspired by Burrowing Worms, 2016 Ieee International Conference on Robotics and Biomimetics (Robio) (2016) 31-38.
[11] T.J. Wallin, J. Pikul, R.F. Shepherd, 3D printing of soft robotic systems, Nat Rev Mater 3(6) (2018) 84-100.
[12] J. Odent, T.J. Wallin, W.Y. Pan, K. Kruemplestaedter, R.F. Shepherd, E.P. Giannelis, Highly Elastic, Transparent, and Conductive 3D-Printed Ionic Composite Hydrogels, Adv Funct Mater 27(33) (2017).
[13] T.J. Wallin, J.H. Pikul, S. Bodkhe, B.N. Peele, B.C. Mac Murray, D. Therriault, B.W. McEnerney, R.P. Dillon, E.P. Giannelis, R.F. Shepherd, Click chemistry stereolithography for soft robots that self-heal, J Mater Chem B 5(31) (2017) 6249-6255.
[14] D.K. Patel, A.H. Sakhaei, M. Layani, B. Zhang, Q. Ge, S. Magdassi, Highly Stretchable and UV Curable Elastomers for Digital Light Processing Based 3D Printing, Adv Mater 29(15) (2017).
[15] R. Matsuzaki, M. Ueda, M. Namiki, T.K. Jeong, H. Asahara, K. Horiguchi, T. Nakamura, A. Todoroki, Y. Hirano, Three-dimensional printing of continuous-fiber composites by in-nozzle impregnation, Sci Rep-Uk 6 (2016).
[16] C.B.K.O. Melenka G.W., Schofield J. S., Dawson M.R., Carey J.P., Evaluation and prediction of the tensile properties of continuous fiber-reinforced 3D printed structures, Composite Structures 153 (2016) 866–875.
[17] NinjaTek. NinjaFlex ® 3D printing filament: flexible polyurethane material for FDM printers. https://ninjatek.com/products/filaments/ninjaflex/.
[18] J.F. Christ, N. Aliheidari, A. Ameli, P. Potschke, 3D printed highly elastic strain sensors of multiwalled carbon nanotube/thermoplastic polyurethane nanocomposites, Materials & Design 131 (2017) 394-401.
[19] T.X. Plott J, Shih AJ. , Voids and tensile properties in extrusion-based additive manufacturing of moisture-cured silicone elastomer, Additive Manufacturing 22 (2018) 606-617.
[20] R.G.I.a. Shannon E. Bakaricha, Reece Gately b, Sina Naficya,c,, b. Marc in het Panhuis a, Geoffrey M. Spinks, 3D printing of tough hydrogel composites with spatially varying materials properties, Additive Manufacturing 14 (2017) 24-30.
[21] J. Morrow, S. Hemleben, Y. Menguc, Directly Fabricating Soft Robotic Actuators With an Open-Source 3-D Printer, Ieee Robot Autom Let 2(1) (2017) 277-281.

[22] O.T. Yirmibeşoğlu OD, Olson G, Palmer C, Mengüç Y. , Evaluation of 3D Printed Soft Robots in Radiation Environments and Comparison with Molded Counterparts, Frontiers in Robotics and AI. 6 (2019) 40.
[23] X. Ren, H. Shao, T. Lin, H. Zheng, 3D gel-printing—An additive manufacturing method for producing complex shape parts, Materials & Design 101 (2016) 80-87.
[24] F. Liravi, E. Toyserkani, Additive manufacturing of silicone structures: A review and prospective, Additive Manufacturing 24 (2018) 232-242.
[25] F. Liravi, E. Toyserkani, A hybrid additive manufacturing method for the fabrication of silicone bio-structures: 3D printing optimization and surface characterization, Materials & Design 138 (2018) 46-61.
[26] S.S. Muthusamy M, Chen RK., Additive Manufacturing of Overhang Structures Using Moisture-Cured Silicone with Support Material, .Journal of Manufacturing and Materials Processing (2.2) (2018) 24.
[27] G.L. Goh, S. Agarwala, W.Y. Yong, 3D printing of microfludic sensor for soft robots: a preliminary study in design and fabrication, the 2nd International Conference on Progress in Additive Manufacturing (Pro-AM 2016), 2016.
[28] N.P. Macdonald, F. Zhu, C. Hall, J. Reboud, P. Crosier, E. Patton, D. Wlodkowic, J. Cooper, Assessment of biocompatibility of 3D printed photopolymers using zebrafish embryo toxicity assays, Lab on a Chip 16(2) (2016) 291-297.
[29] T.J. Hinton, A. Hudson, K. Pusch, A. Lee, A.W. Feinberg, 3D Printing PDMS Elastomer in a Hydrophilic Support Bath via Freeform Reversible Embedding, Acs Biomater Sci Eng 2(10) (2016) 1781-1786.
[30] D.S. Kim, B.L. Tai, Hydrostatic support-free fabrication of three-dimensional soft structures, Journal of Manufacturing Processes 24 (2016) 391-396.
[31] C.S. O'Bryan, T. Bhattacharjee, S. Hart, C.P. Kabb, K.D. Schulze, I. Chilakala, B.S. Sumerlin, W.G. Sawyer, T.E. Angelini, Self-assembled micro-organogels for 3D printing silicone structures, Sci Adv 3(5) (2017).
[32] M. Wehner, R.L. Truby, D.J. Fitzgerald, B. Mosadegh, G.M. Whitesides, J.A. Lewis, R.J. Wood, An integrated design and fabrication strategy for entirely soft, autonomous robots, Nature 536(7617) (2016) 451.
[33] M.A. Skylar-Scott, S.G. Uzel, L.L. Nam, J.H. Ahrens, R.L. Truby, S. Damaraju, J.A. Lewis, Biomanufacturing of organ-specific tissues with high cellular density and embedded vascular channels, Science advances 5(9) (2019) eaaw2459.
[34] M.J. Yirmibesoglu OD, Walker S, Gosrich W, Cañizares R, Kim H, Daalkhaijav U, Fleming C, Branyan C, Menguc Y, Direct 3D printing of silicone elastomer soft robots and their performance comparison with molded counterparts, IEEE International Conference on Soft Robotics (RoboSoft) IEEE, 2018.
[35] J. Plott, and Albert Shih, The extrusion-based additive manufacturing of moisture-cured silicone elastomer with minimal void for pneumatic actuators., Additive Manufacturing 17 (2017) 1-14.
[36] S. Walker, U. Daalkhaijav, D. Thrush, C. Branyan, O.D. Yirmibesoglu, G. Olson, Y. Menguc, Zero-Support 3D Printing of Thermoset Silicone Via Simultaneous Control of Both Reaction Kinetics and Transient Rheology, 3d Print Addit Manuf 6(3) (2019) 139-147.
[37] F.C. Godoi, S. Prakash, B.R. Bhandari, 3d printing technologies applied for food design: Status and prospects, J Food Eng 179 (2016) 44-54.
[38] X. Song, Z.F. Zhang, Z.Y. Chen, Y. Chen, Porous Structure Fabrication Using a Stereolithography-Based Sugar Foaming Method, J Manuf Sci E-T Asme 139(3) (2017).
[39] D.B. Kolesky, R.L. Truby, A.S. Gladman, T.A. Busbee, K.A. Homan, J.A. Lewis, 3D Bioprinting of Vascularized, Heterogeneous Cell-Laden Tissue Constructs, Adv Mater 26(19) (2014) 3124-3130.
[40] M.C. Gryka, T. Comi, R.A. Forsyth, P.M. Hadley, S. Deb, R. Bhargava, Controlled dissolution of freeform 3D printed carbohydrate glass scaffolds in hydrogels using a hydrophobic spray coating, Additive Manufacturing 26 (2019) 193-201.

[41] A. Begin-Drolet, M.A. Dussault, S.A. Fernandez, J. Larose-Dutil, R.L. Leask, C.A. Hoesli, J. Ruel, Design of a 3D printer head for additive manufacturing of sugar glass for tissue engineering applications, Additive Manufacturing 15 (2017) 29-39.
[42] L.M. Bellan, S.P. Singh, P.W. Henderson, T.J. Porri, H.G. Craighead, J.A. Spector, Fabrication of an artificial 3-dimensional vascular network using sacrificial sugar structures, Soft Matter 5(7) (2009) 1354-1357.
[43] J.S. Miller, K.R. Stevens, M.T. Yang, B.M. Baker, D.H.T. Nguyen, D.M. Cohen, E. Toro, A.A. Chen, P.A. Galie, X. Yu, R. Chaturvedi, S.N. Bhatia, C.S. Chen, Rapid casting of patterned vascular networks for perfusable engineered three-dimensional tissues, Nat Mater 11(9) (2012) 768-774.
[44] Y. He, J.J. Qiu, J.Z. Fu, J. Zhang, Y.N. Ren, A. Liu, Printing 3D microfluidic chips with a 3D sugar printer, Microfluid Nanofluid 19(2) (2015) 447-456.
[45] H.G. Gelber MK, Comi TJ, Bhargava R, Model-guided design and characterization of a high-precision 3D printing process for carbohydrate glass, Additive Manufacturing 22 (2018) 38-50.
[46] P.Y.V. Leung, Sugar 3D Printing: Additive Manufacturing with Molten Sugar for Investigating Molten Material Fed Printing, 3d Print Addit Manuf 4(1) (2017) 13-17.
[47] J. Gopinathan, I. Noh, Recent trends in bioinks for 3D printing, Biomaterials research 22(1) (2018) 11.
[48] Y. Tadesse, Moore, D., Thayer, N. and Priya, S., Silicone based artificial skin for humanoid facial expressions, Electroactive Polymer Actuators and Devices (EAPAD) International Society for Optics and Photonics., 2009.
[49] A.a.T. Hamidi, Y., Single step 3D printing of bioinspired structures via metal reinforced thermoplastic and highly stretchable elastomer, Composite Structures 210 (2019) 250-261.
[50] A. Hamidi, S. Jain, Y. Tadesse, 3D printing PLA and silicone elastomer structures with sugar solution support material, Proc Spie 10163 (2017).
[51] Y.H. Roos, M. Karel, Plasticizing Effect of Water on Thermal-Behavior and Crystallization of Amorphous Food Models, J Food Sci 56(1) (1991) 38-43.
[52] T.S. Lumpe, J. Mueller, K. Shea, Tensile properties of multi-material interfaces in 3D printed parts, Materials & Design 162 (2019) 1-9.
[53] Y. Zhang, The effect of surface roughness parameters on contact and wettability of solid surfaces, (2007).
[54] Y. He, G.H. Xue, J.Z. Fu, Fabrication of low cost soft tissue prostheses with the desktop 3D printer, Sci Rep-Uk 4 (2014).
[55] Standard Test Methods for Vulcanized Rubber and Thermoplastic Elastomers—Tension1, 2009. http://www.univstrut.com/uploadfiles/pdf/3.pdf.
[56] S. Cantournet, R. Desmorat, J. Besson, Mullins effect and cyclic stress softening of filled elastomers by internal sliding and friction thermodynamics model, International Journal of Solids and Structures 46(11-12) (2009) 2255-2264.
[57] K. Mojsiewicz-Pienkowska, M. Jamrogiewicz, K. Szymkowska, D. Krenczkowska, Direct Human Contact with Siloxanes (Silicones) - Safety or Risk Part 1. Characteristics of Siloxanes (Silicones), Front Pharmacol 7 (2016).
[58] R.W. Hartel, R. Ergun, S. Vogel, Phase/State Transitions of Confectionery Sweeteners: Thermodynamic and Kinetic Aspects, Compr Rev Food Sci F 10(1) (2011) 17-32.

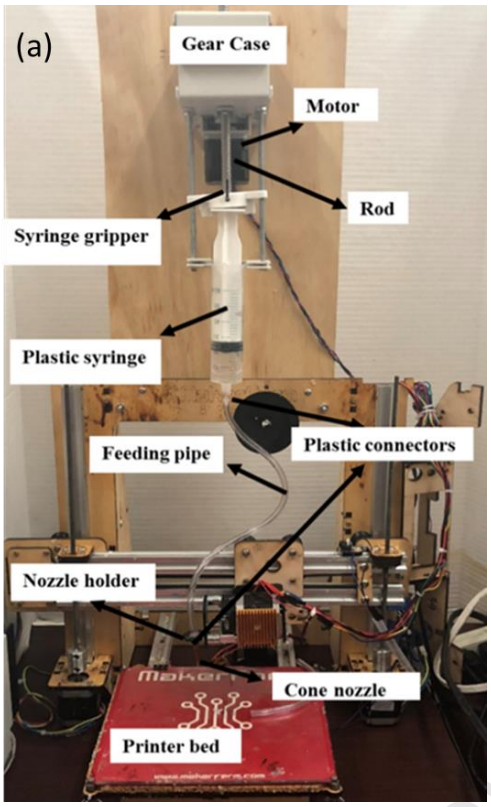

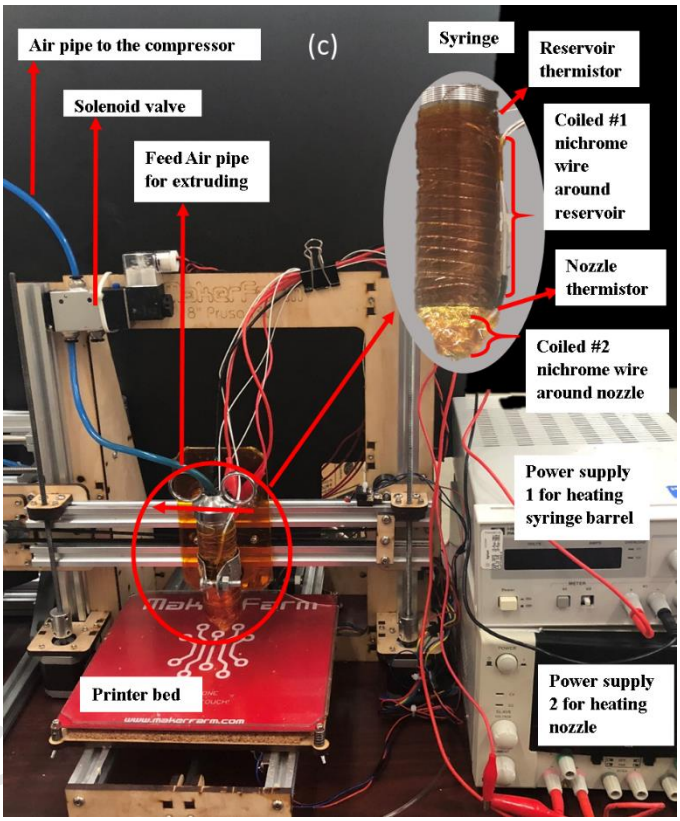

Figures:

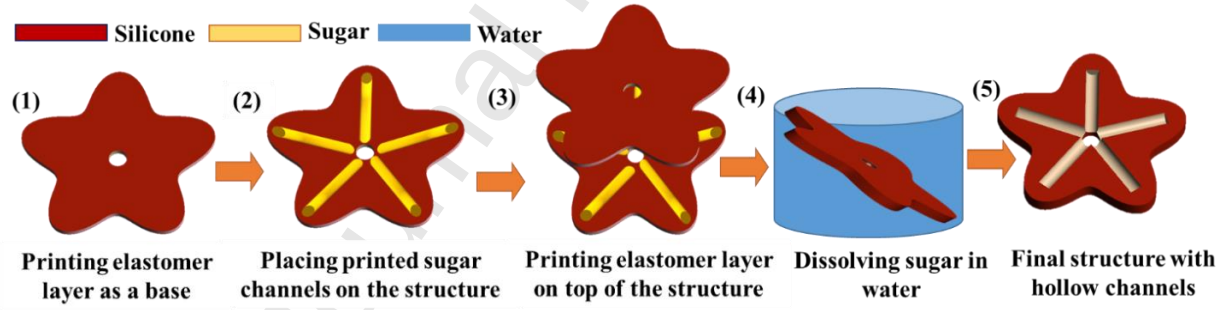

Figure 1. Steps for fabricating a soft pneumatic actuator using a 3D printed sugar structure as support material.

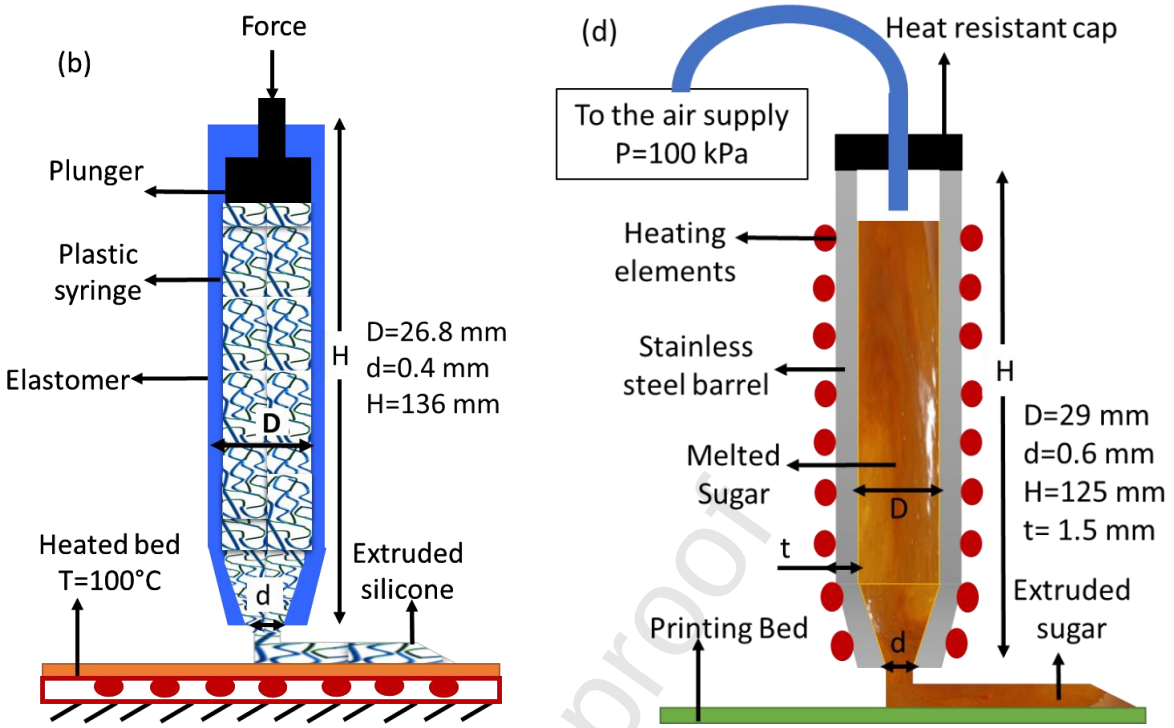

Figure 2. (a)3D printer setup for elastomer, (c)schematic of extruder for printing elastomer, (c)3D printer setup for carbohydrate glass, and (d)schematic of extruder for printing carbohydrate glass.

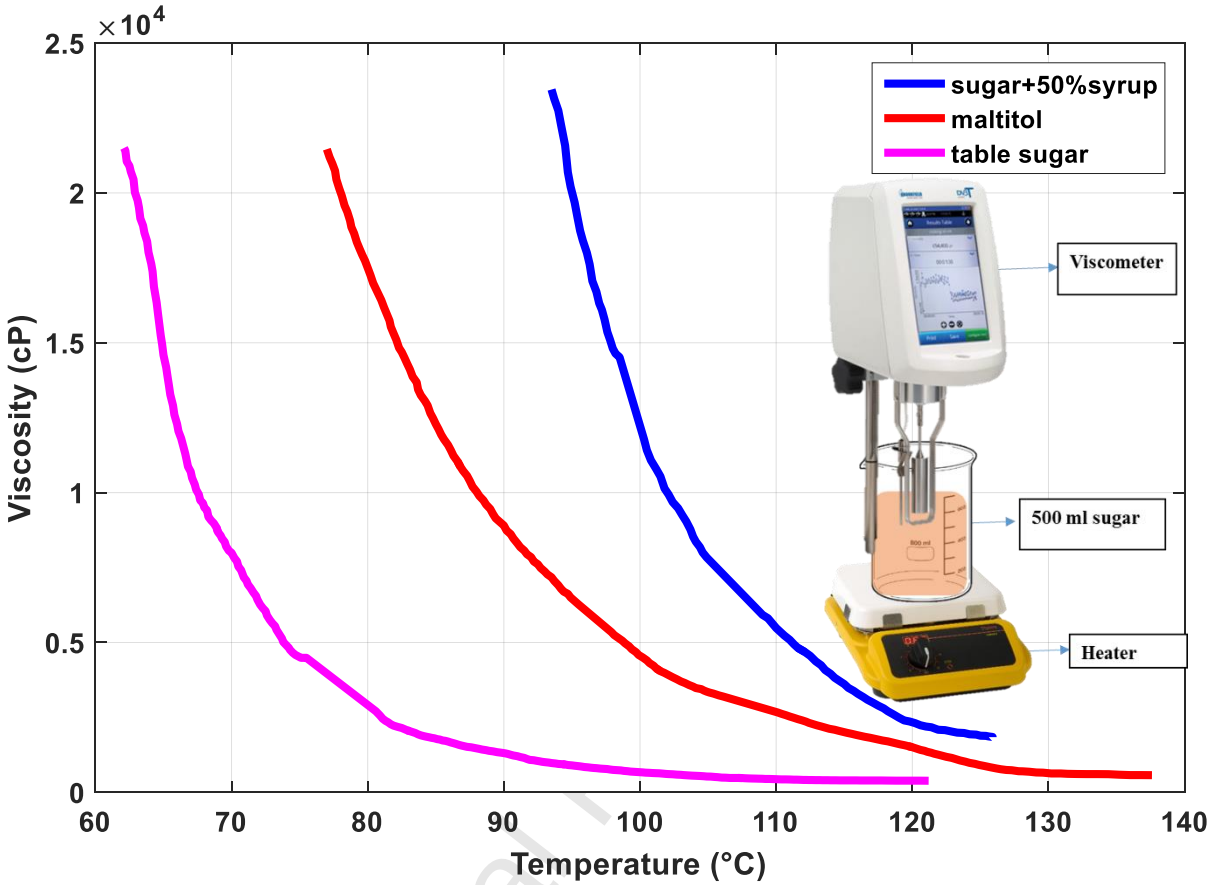

Figure 3. Viscosity measurement of maltitol and the mixture of sugar and syrup at different temperatures (higher range of viscosity was not measured due to the limitation of viscometer).

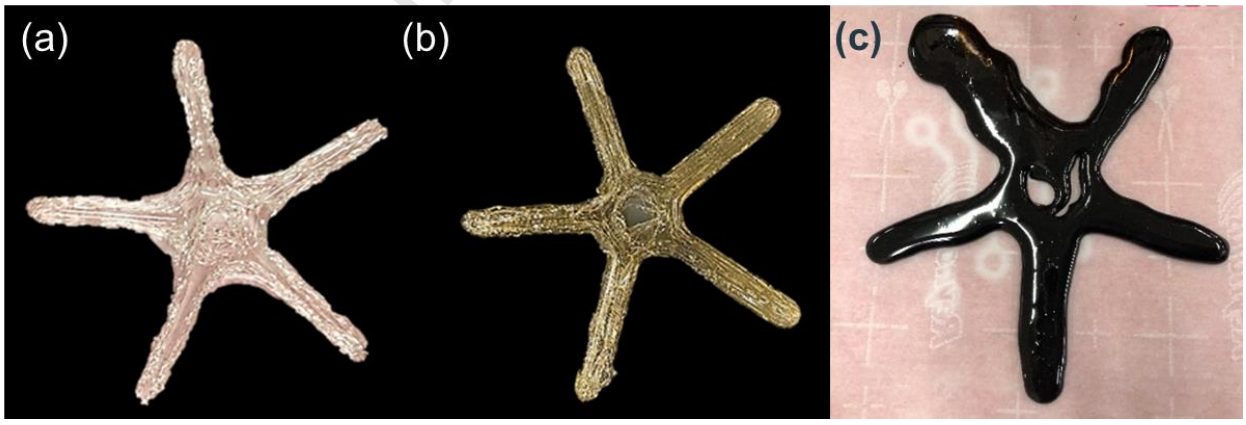

Figure 4. 3D printed structure by: (a)molten maltitol at 154 ˚C, (b)reheating maltitol (maltitol) at 154˚C and (c)reheating maltitol for an hour at 154˚C. In this case, the carbohydrate oxidized and the color changed to black.

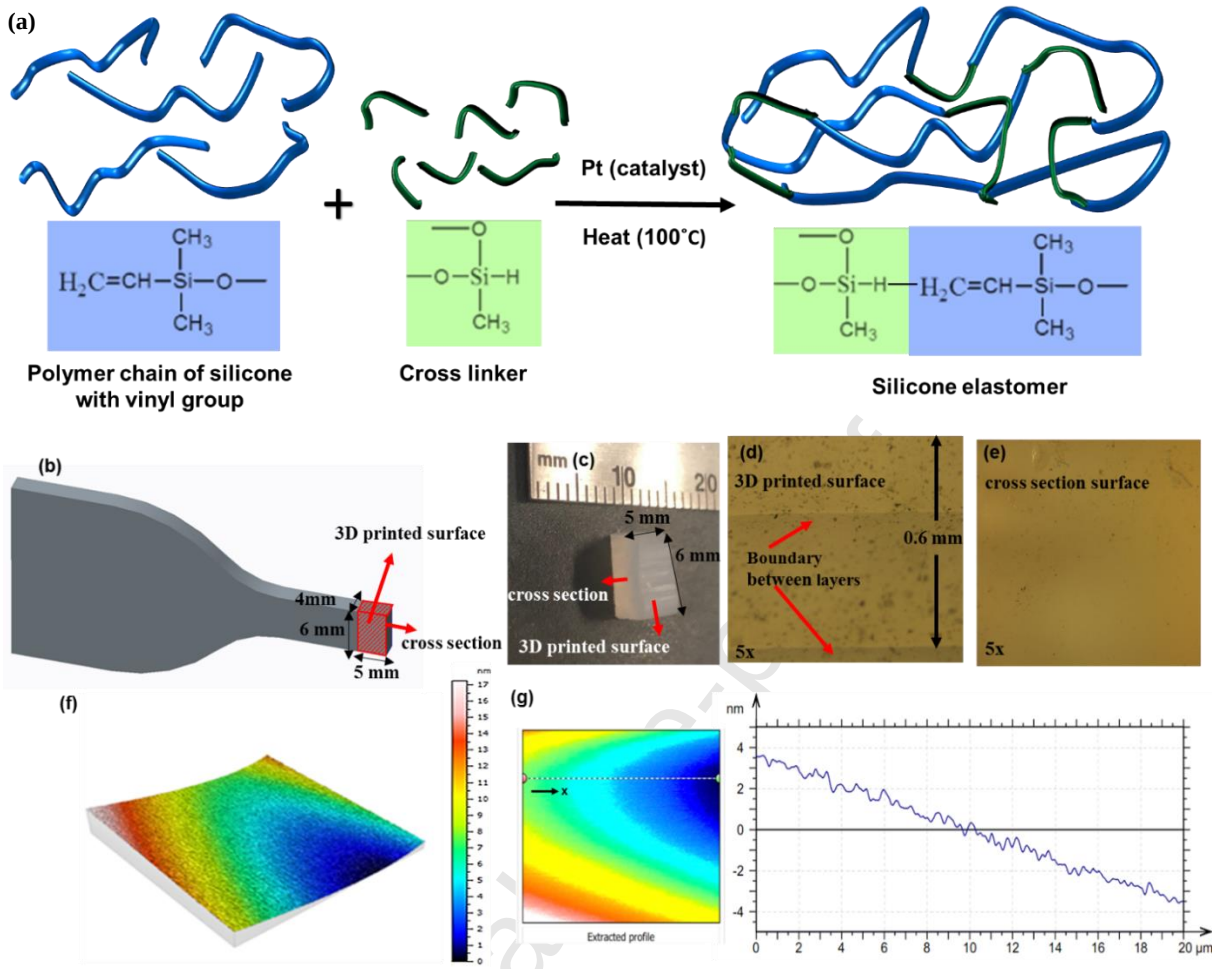

Figure 5. Characterization of Ecoflex 0010: (a)chemical reaction of platinum cured silicone [57], (b)section of the 3D printed dog bone sample studied by microscopic images, (c)image of the 3D printed sample studied by microscopic images, (d)microscopic image of 3D printed silicone surface (6x5mm), (e)microscopic image of cross section surface (6×4 mm), (h)AFM image of the surface of 3D printed silicone, and (g)extracted profile for calculating surface roughness.

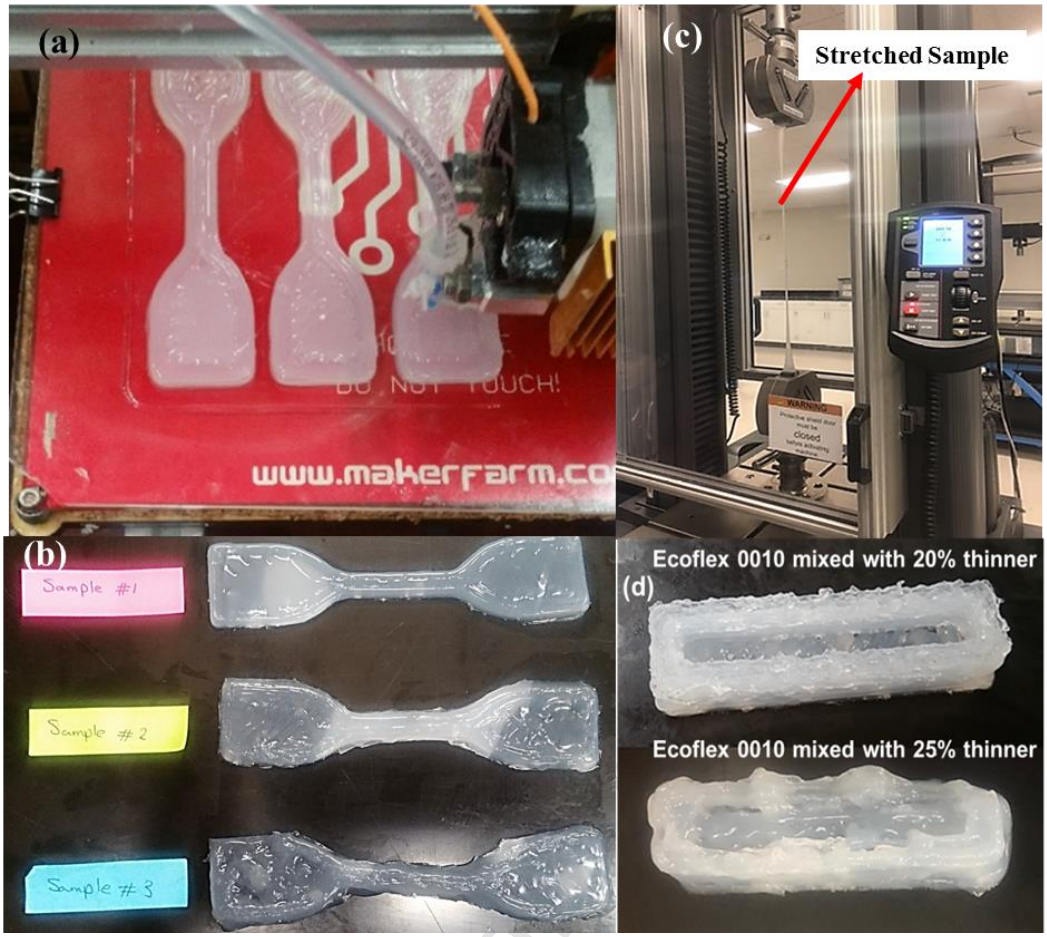

Figure 6. 3D printed Ecoflex 0010 samples: (a)3D printing samples for tensile test, (b)3D printed dog bone sample with 20% (sample#1), 25% (sample#2) and 18%(sample#3) thinner, (c)tensile test of silicone sample and (d)3D printed silicone chamber by Ecoflex 0010 mixed with 20% (up) and 25% (down) thinner.

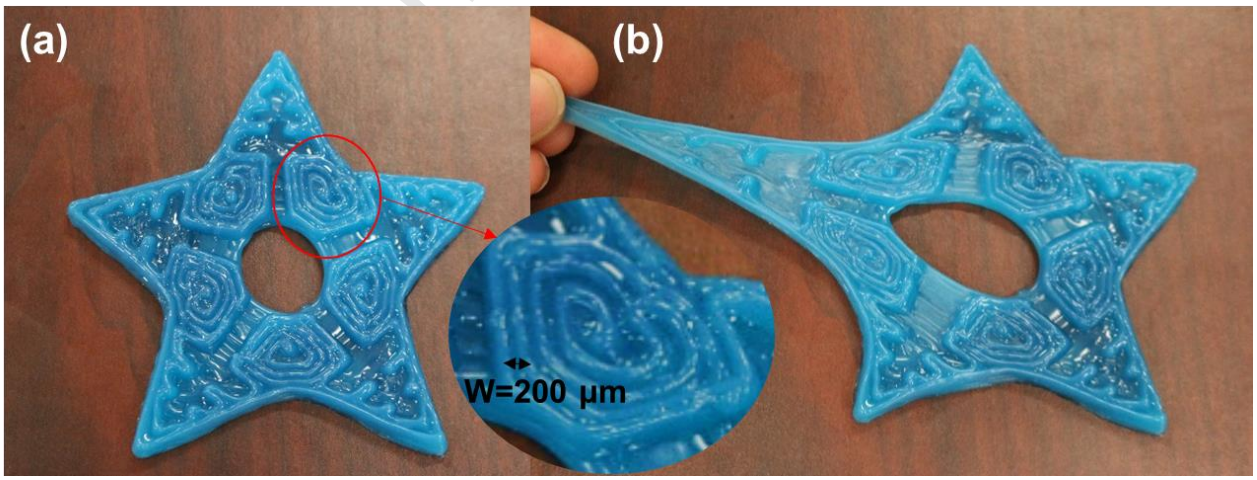

Figure 7. 3D printed highly stretchable structure with the complex internal pattern: (a)3D printed structure with 200 µm channels and (b)flexibility of the structure (video S2).

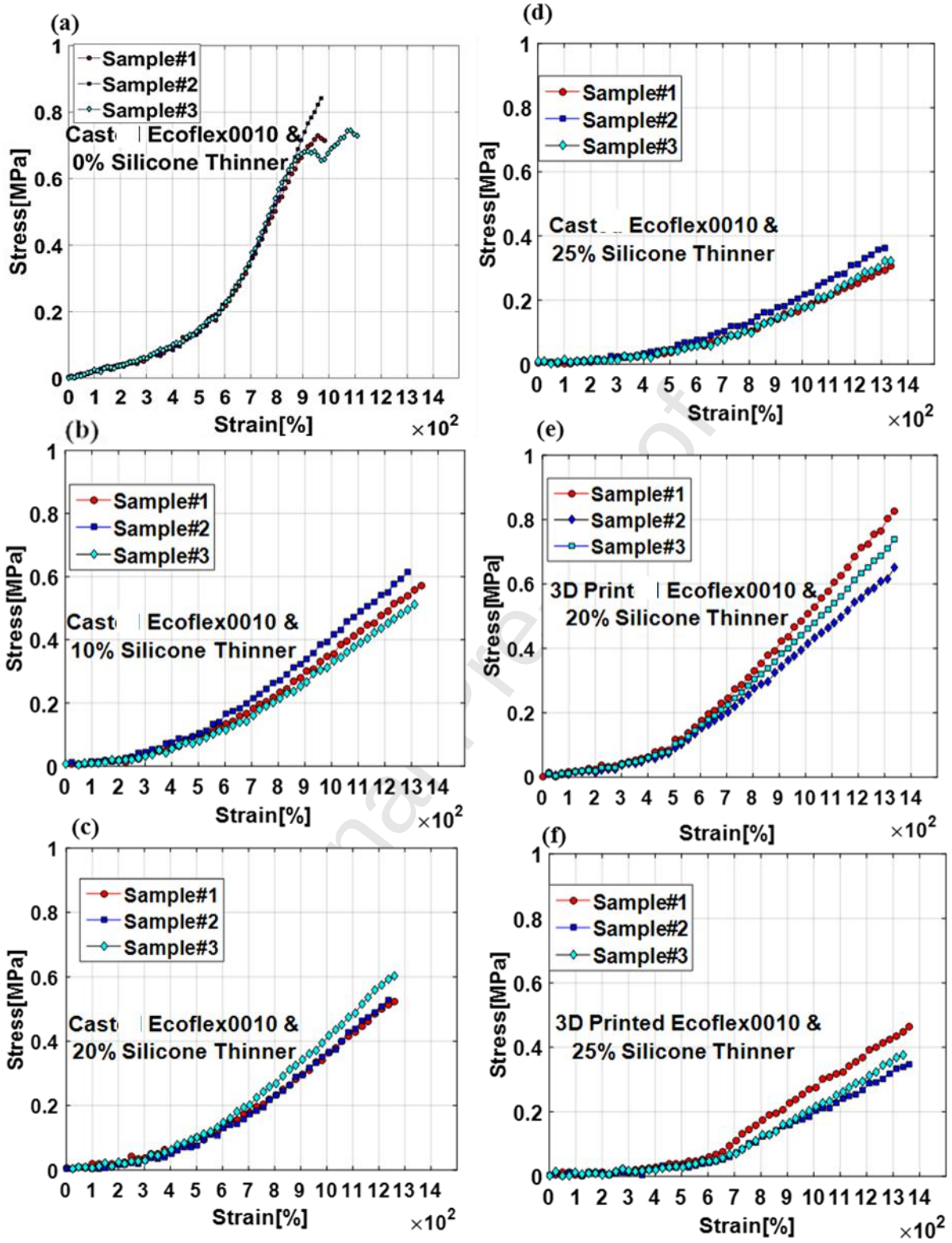

Figure 8. Comparison of tensile strength and strain of Ecoflex 0010: (a)cast with 0% silicone thinner, (b)cast with 10% silicone thinner, (c)casted with 20% silicone thinner, (d)cast with 25% silicone thinner, (e)3D printed with 20% silicone thinner, and (f)3D printed with 25% silicone thinner.

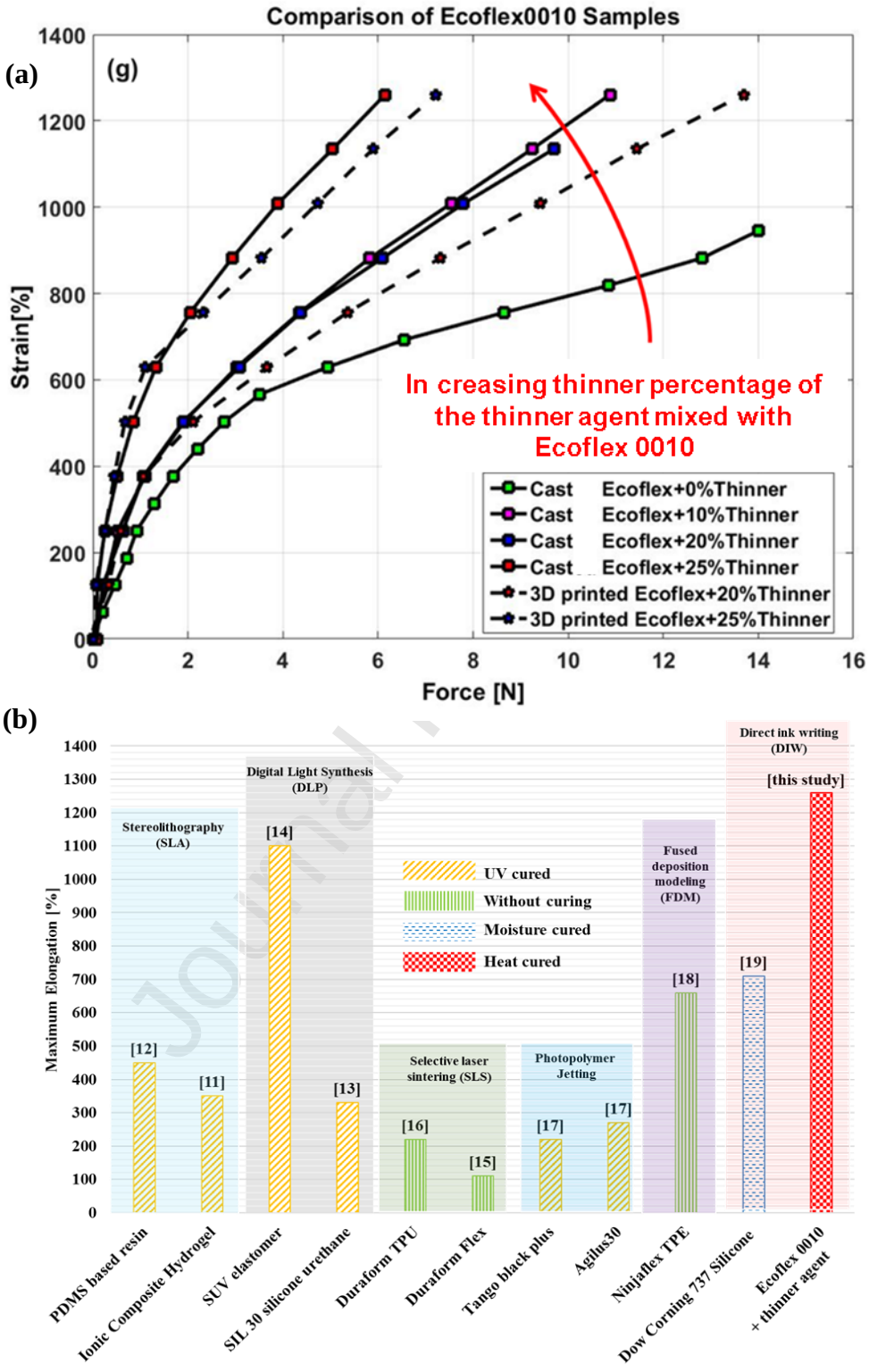

Figure 9. (a)Comparison of elongation versus force for Ecoflex 0010 samples mixed with different percentage of the thinner agent, (b)comparison between the maximum deformation of 3D printed soft materials reported in ref.[12-19] and this study.

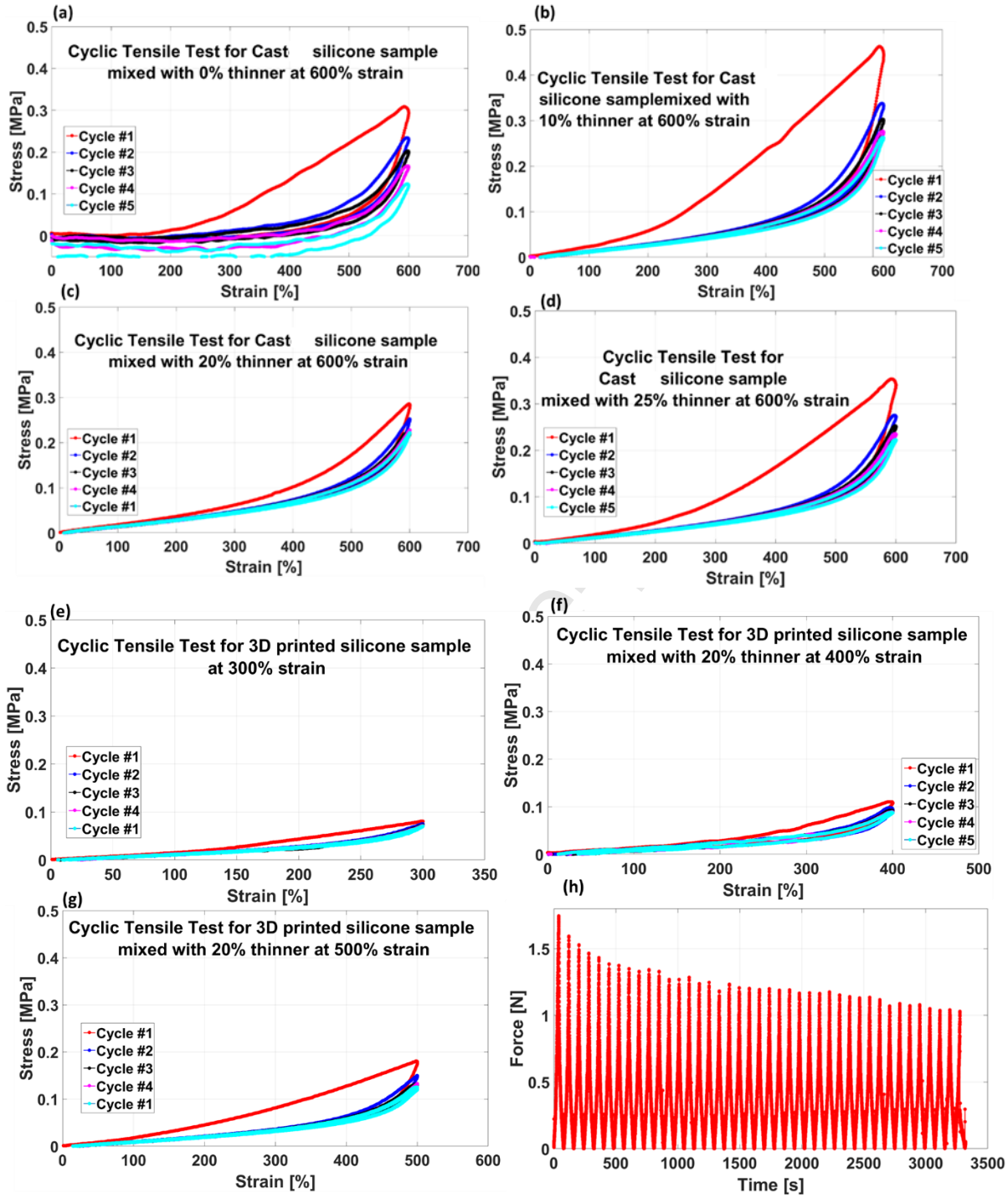

Figure 10 Uniaxial cyclic response of cast silicone samples with: (a)0% thinner, (b)10% thinner, (c) 20% thinner and (d)25% thinner. Uniaxial cyclic response of 3D printed silicone samples at: (e)300% strain, (f)400% strain, (g)500% strain and cyclic loading and unloading for 3D printed Ecoflex 0010 sample with 20% thinner where the sample stretched 4 times its original length at each cycle. The samples did not fail until the 40th cycle.

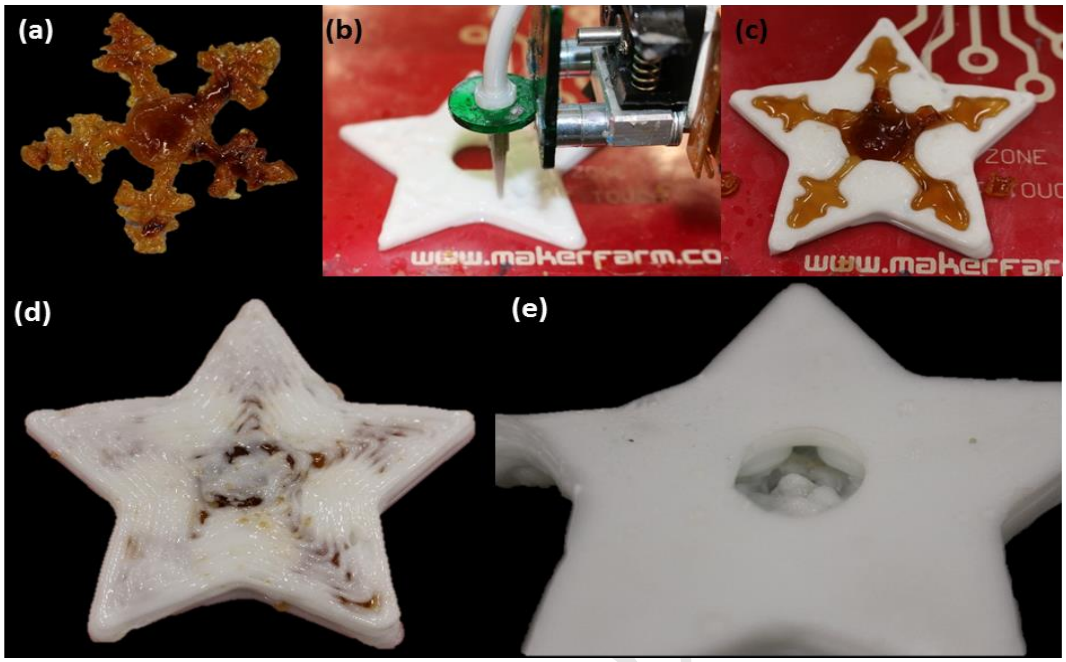

Figure 11. 3D printing procedure of a silicone structure with hollow channels using carbohydrate glass: (a)3D printed carbohydrate glass (sugar and 50% syrup) (b)3D printed silicone structure, (c)3D printed carbohydrate glass inserted in the soft structure, (d)a layer of silicone 3D printed on top of the carbohydrate glass and (e)channel formed inside silicone after dissolving the carbohydrate glass in water.

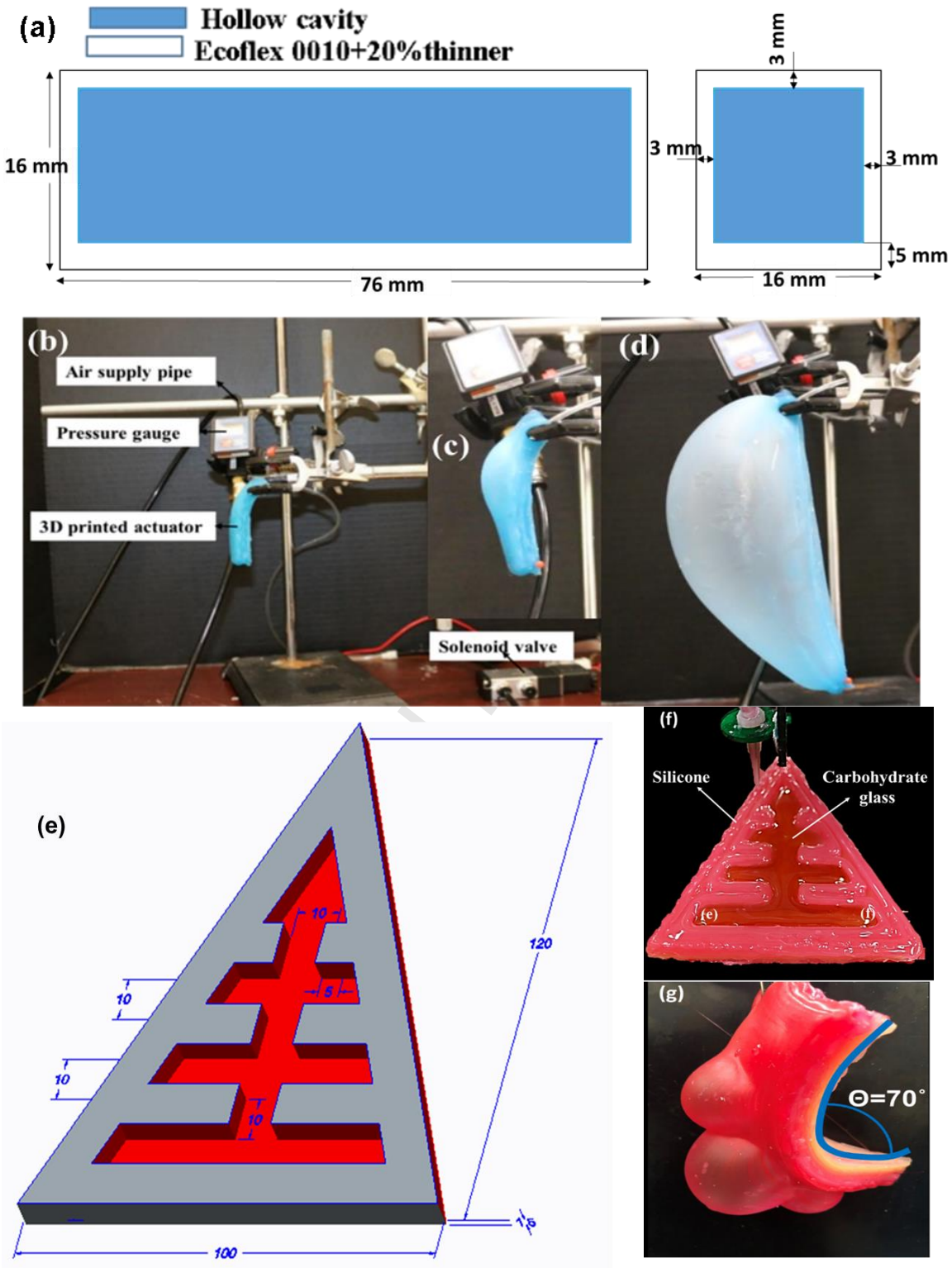

Figure 12. 3D printed single elastomer chamber with the use of carbohydrate glass as sacrificial material: (a)design of the chamber, (b)pressure test setup, (c)3D printed pneumatic actuator (using carbohydrate glass) started actuating and (d)deformation at 70 kPa. 3D printed fluidic actuator with silicone and carbohydrate glass: (e)design, (f)3D printing soft structure, (g)fluidic actuation.

Tables:

3D Printed Ecoflex 0010		**Carbohydrate glass (maltitol)**	
Nozzle Diameter	0.4 mm	Nozzle Diameter	0.6 mm
Layer Thickness after curing	0.5 mm	Layer Thickness	1.1 mm
Nozzle Temperature	25˚C (room temperature)	Nozzle Temperature	110-120˚C
Print Bed Temperature	100 ˚C	Print Bed Temperature	25 ˚C (room temperature)
Head translation speed for the first layer	15 mm/s	Head translation speed for the first layer	10 mm/s
Head Translation Speed for all layers (except the first layer)	15 mm/s	Head Translation Speed for all layers (except the first layer)	5-10 mm/s
Layer height	0.43 mm	Layer height	0.6 mm
Infill density	100%	Infill density	90%

Table 1. 3D printing parameters for printing silicone and carbohydrate glass.

Table 2. Glass transition temperature T_g and melting temperature T_m of carbohydrate glass [40, 58].

Types of sugar	T_g (˚C)	T_m (˚C)
Sucrose	62-70	186
Maltose	87	110
Maltitol	39	145-152
Glucose	31	146-150
Fructose	5-10	103-105
Lactitol	52-58	146
Sorbitol	-9	95
Erythritol	-59.7	121
Xylitol	-29	94
Mannitol	13	166-168
Isomalt	63.6	145-150

Declaration of interests

☒ The authors declare that they have no known competing financial interests or personal relationships that could have appeared to influence the work reported in this paper.

☐The authors declare the following financial interests/personal relationships which may be considered as potential competing interests:

3D printing of very soft elastomer and sacrificial carbohydrate glass/elastomer structures for robotic applications

Armita Hamidi[1] and Yonas Tadesse[2]

[1]armita.hamidi@utdallas.edu, [2]Yonas.Tadesse@utdallas.edu,

Humanoid, Biorobotics and Smart Systems (HBS Lab)
Mechanical Engineering Department,
Erik Jonsson School of Engineering and Computer Science,
The University of Texas at Dallas (UTD),
800 West Campbell Rd., Richardson, TX75080-3021

Highlights

- Material processing parameters for a new AM process that allows the fabrication of highly elastic soft structures are presented.
- 3D printing silicone samples with 20% thinner resulted in an ultimate tensile elongation of 1260 %
- Extensive material characterization results for the 3D printed soft materials including tensile test, cyclic test, optical microscopy and atomic force microscopy are presented.
- Soft hydraulic/pneumatic actuators are fabricated via 3D printing carbohydrate glass and soft silicone elastomer, for ultimate application in soft robots.